Unequal Bandwidth Spectral Analysis using Digital Frequency Warping

CARLO BRACCINI AND ALAN V. OPPENHEIM, SENIOR MEMBER, IEEE

Abstract—**The application to unequal bandwidth and vernier spectrum analysis of a technique referred to as digital frequency warping is discussed. In this technique a sequence is transformed in such a way that the Fourier transforms of the original and transformed sequences are related by a nonlinear transformation of the frequency axis. An equal bandwidth analysis carried out on the transformed sequence then corresponds to an unequal bandwidth analysis of the original sequence.**

A comparison is presented between the bandwidth as a function of frequency for the digital warping technique and proportional bandwidth analysis. An analysis of the effects of finite register length in implementing digital frequency warping is also presented.

I. INTRODUCTION

SPECTRAL analysis has traditionally played an important role in the more general area of signal processing. With the development of the fast Fourier transform (FFT) algorithm and the present trend in digital hardware it has become increasingly practical to carry out sophisticated spectral analysis digitally [1].

In its most straightforward application in digital spectral analysis, the use of the FFT corresponds to an analysis carried out with a filter bank with equal bandwidth filters uniformly spaced over the entire signal band [2]. In many spectral analysis applications, however, it is desirable to have the analysis bandwidth change with frequency. For example, in the analysis of noise generated by mechanical systems for detecting potential failures it is often important to utilize proportional bandwidth or constant Q analysis so that the form of the spectrum is invariant under a time scaling of the signal resulting, for example, from a change in speed of the system. Such an analysis has been referred to as a form invariant spectral analysis [3]. In other instances, it is desirable to analyze wide bandwidth data while obtaining high resolution at the low frequencies. In this case, it is generally desired to have the analysis bandwidth increase with frequency but the exact form of the bandwidth as a function of frequency is not crucial.

Another example of what can be regarded as spectral analysis with an analysis bandwidth which is frequency dependent is a vernier analysis. In this case, we are interested in an analysis over a small portion of the band, with the effective filter spacing much smaller than the effective filter width or with the filter bandwidth much smaller than the spectral resolution available in the data so that the spectrum is oversampled in frequency. Such an analysis is often useful when one is interested in detecting and measuring the center frequency of a narrowband component with a simple peak-picking algorithm on the spectrum. This corresponds to a very fine spectral sampling in a part of the frequency band, and none or very low spectral sampling in the remainder of the band. One procedure for obtaining a vernier spectral analysis is to implement a high-order discrete Fourier transform (DFT). This results in a fine spectral sampling over the entire frequency band and is therefore inefficient. Another procedure which has been used utilizes the chirp z-transform algorithm [4].

In this paper, the application of a technique referred to as digital frequency warping to unequal bandwidth spectral analysis will be discussed. This technique transforms a sequence in such a way that the Fourier transforms of the original and transformed sequences are related by a nonlinear transformation of the frequency axis. An equal bandwidth analysis carried out on the transformed sequence then corresponds to an unequal bandwidth analysis of the original sequence. While the class of frequency transformations afforded by this technique does not permit proportional bandwidth analysis, it does permit an analysis in which the analysis bandwidth increases or decreases with frequency and also permits a vernier analysis.

In the following discussion, we will present a framework for discussing the problem of spectral analysis. We will then discuss in a general sense how unequal bandwidth spectral analysis can be implemented by first implementing a nonlinear distortion of the frequency axis, followed by an unequal bandwidth analysis. We then apply these ideas to the specific class of frequency transformations implementable with the digital frequency warping technique, in particular, comparing the bandwidth versus frequency with a proportional bandwidth analysis.

One of the potential advantages of digital frequency warping lies in its relatively simple hardware implementation. This implementation corresponds basically to a cascade chain of first-order digital filters and thus, an important

Manuscript received August 21, 1973; revised December 28, 1973. This work was supported in part by the Italian C.N.R. (National Council of Research), National Science Foundation under Grant GK-31353, and the Advanced Research Projects Agency monitored by the ONR under Contract N 00014-67-A-0204-0064.

C. Braccini was with the Research Laboratory of Electronics, Massachusetts Institute of Technology, Cambridge, Mass. 02173. He is now with the Istituto di Elettrotecnia dell'Universita di Genova, Genova, Italy.

A. V. Oppenheim is with the Department of Electrical Engineering and Research Laboratory of Electronics, Massachusetts Institute of Technology, Cambridge, Mass. 02173.

consideration in the use of this technique is its sensitivity to arithmetic roundoff noise. Thus, we conclude the paper with an analysis of these effects.

II. GENERAL SPECTRAL ANALYSIS

Let $f(n)$ denote a sequence of data and $F(\Omega)$ its Fourier transform. A set of measurements of the spectrum as viewed through a spectral window will be denoted by G_k with[1]

$$G_k = \left| \int_{-\pi}^{\pi} F(\Omega) H(\Omega,\Omega_k)\, d\Omega \right|; \qquad k = 1,2,\cdots,N. \quad (1)$$

The fact that the spectral window $H(\Omega,\Omega_k)$ is a function of two variables indicates that the shape and in particular, the width of the window can change with the center frequency Ω_k. When the spectral window $H(\Omega,\Omega_k)$ depends only on the difference $(\Omega - \Omega_k)$ (1) becomes

$$G_k = \left| \int_{-\pi}^{\pi} F(\Omega) H(\Omega - \Omega_k)\, d\Omega \right|, \quad (2)$$

and equal bandwidth analysis results. The spectral measurements G_k can be thought of as corresponding qualitatively to filter bank outputs where each filter has the same spectral shape with only the center frequency Ω_k changing along the filter bank. Generally, it is desirable to choose the low-pass prototype filter characteristic $H(\Omega)$ to approximate unity over a band of frequencies with a width which we will denote by B and zero outside the band and to choose the spacing of the center frequencies, i.e., $(\Omega_{k+1} - \Omega_k)$ to equal the constant B independent of k. In this way, the band is covered by nonoverlapping filters. Alternatively, for vernier analysis the spacing of the center frequencies is chosen to be much less than the filter width.

If the spectral analysis corresponds to proportional bandwidth analysis then (1) takes the form

$$G_k = \left| \int_{-\pi}^{\pi} F(\Omega) H\left(\frac{\Omega}{\Omega_k}\right) d\Omega \right|. \quad (3)$$

In this case, the effective filter width is proportional to the center frequency. Here the effective filters become wider as the center frequency increases.

Generally, when data are analyzed using the DFT, a finite length window $w(n)$ is applied to the data and the DFT of the product computed. The magnitude of the DFT values then correspond to spectral samples G_k as specified by (2) with $\Omega_k = k\Omega_0$. The Fourier transform of the data window $w(n)$ corresponds to the spectral window $H(\Omega)$. Thus, a direct application of the DFT results in an equal resolution analysis. A commonly used procedure for approximating a constant Q analysis or more generally unequal resolution is to sum adjacent measurements G_k's obtained via DFT, with the number of bins summed increasing with frequency. This first requires, of course, a DFT calculation of sufficiently high order.

[1] Throughout this paper we will use a normalized frequency scale so that with a sampling period of T, the sampling frequency $2\pi/T$ corresponds to $\Omega = 2\pi$.

III. UNEQUAL BANDWIDTH SPECTRUM ANALYSIS BASED ON FREQUENCY TRANSFORMATION

The DFT computes spectral samples whose magnitude is of the form

$$G_k = \left| \int_{-\pi}^{\pi} F(\Omega) H(\Omega - k\Omega_0)\, d\Omega \right| \quad (4)$$

corresponding to an equal bandwidth analysis of $f(n)$. Let us consider a sequence $\hat{f}(n)$ which is related to $f(n)$ in such a way that

$$F(\Omega) = \hat{F}(\hat{\Omega}) \quad (5)$$

where $\hat{\Omega} = \theta(\Omega)$. An equal resolution analysis of $\hat{F}(\hat{\Omega})$ according to (4) leads to the coefficients

$$\hat{G}_k = \left| \int_{-\pi}^{\pi} \hat{F}(\hat{\Omega}) H(\hat{\Omega} - k\hat{\Omega}_0)\, d\hat{\Omega} \right| \quad (6)$$

or, since $\hat{\Omega} = \theta(\Omega)$,

$$\hat{G}_k = \left| \int_{-\pi}^{\pi} F(\Omega) H(\theta(\Omega) - \Omega_k) \left(\frac{d\theta(\Omega)}{d\Omega}\right) d\Omega \right| \quad (7)$$

with $\Omega_k = k\theta(\Omega_0)$. This no longer has the form of an equal resolution analysis but, except for the factor $d\theta(\Omega)/d\Omega$, still retains the general form of (1). Thus, we can interpret (7) as an unequal resolution analysis of $f(n)$ modified by the frequency characteristic $d\theta/d\Omega$. This spectral weighting can be compensated for prior to the spectral analysis by means of an appropriate preemphasis, or can be taken into account in interpreting the spectral coefficients. The correction is particularly simple when $\theta(\Omega)$ is close to linear since it reduces to a constant spectral weight.

If the low-pass filter $H(\Omega)$ has a bandwidth B, and if we assume that $\theta(\Omega)$ is approximately linear over any interval of length B, then the bandwidth of $H[\theta(\Omega) - k\theta(\Omega_0)]$ is B divided by the slope of $\theta(\Omega)$ at $\theta(\Omega) = k\theta(\Omega_0)$. Thus, if $\theta(\Omega)$ has slope monotonically decreasing with Ω, then the bandwidth of the analysis will monotonically increase with Ω.

If $\theta(\Omega)$ is linear with slope $\theta'(\Omega) > 1$ in a range of frequencies, then a vernier analysis can be achieved over that range, with bandwidth depending on B and the slope $\theta'(\Omega)$. For a given B, the steeper $\theta(\Omega)$, the finer the analysis.

For the specific case in which we would like a constant percentage bandwidth analysis, $\theta(\Omega)$ is of the form

$$\theta(\Omega) = a_1 \ln a_2\Omega \quad (8)$$

so that (7) takes the form

$$\hat{G}_k = \left[\int_{-\pi}^{\pi} F(\Omega) H\left(a_1 \ln \frac{\Omega}{\Omega_k}\right) \frac{a_1}{\Omega}\, d\Omega \right] \quad (9a)$$

where

$$\Omega_k = a_2^{(k-1)}\Omega_0^k. \tag{9b}$$

There is not available a simple procedure for modifying a sequence to obtain a logarithmic frequency transformation of the form of (8). However, a procedure has been developed for obtaining a frequency transformation of a specific form. In the next section, we briefly review this procedure and then discuss its use for unequal resolution analysis. As a measure of the behavior of the resolution as a function of frequency, we compare it with constant percentage bandwidth.

IV. FREQUENCY WARPING USING AN ALL-PASS TRANSFORMATION

A procedure for implementing a frequency transformation of the form

$$\theta(\Omega) = (\Omega - \Omega_a) + 2\arctan\left(\frac{a\sin(\Omega - \Omega_a)}{1 - a\cos(\Omega - \Omega_a)}\right) \tag{10}$$

has been discussed [5], [6]. The frequency warping achieved is restricted to the functional form of (10) and can only be varied within the flexibility afforded by the parameters a and Ω_a. A plot of $\theta(\Omega)$ for $\Omega_a = 0$ and several values of a is depicted in Fig. 1.

To implement this frequency warping, we consider two sequences $f(n)$ and $\hat{f}(n)$ with Fourier transforms related by

$$F[\exp(j\Omega)] = \hat{F}\{\exp[j\theta(\Omega)]\}.$$

With $\theta(\Omega)$ of the form of (10), and assuming that $f(n)$ is zero for $n < 0$, it has been shown [6] that $f(n)$ and $\hat{f}(n)$ can be related by

$$\hat{f}(k) = \sum_{n=0}^{\infty} \exp(-j\Omega_a n) f(n) h_k(n) \tag{11}$$

where $H_k(z)$, the z-transform of $h_k(n)$ is given by

$$H_k(z) = \begin{cases} \dfrac{(1-a^2)z^{-1}}{(1-az^{-1})^2}\left(\dfrac{z^{-1}-a}{1-az^{-1}}\right)^{k-1} & k > 0 \\ \dfrac{1}{1-az^{-1}} & k = 0. \end{cases} \tag{12}$$

This corresponds to processing $f(-n)\exp(j\Omega_a n)$ with the system shown in Fig. 2. The sequence $\hat{f}(n)$ is obtained by sampling the outputs along the cascade chain at $n = 0$, i.e.,

$$\hat{f}(n) = \tilde{g}_k(0). \tag{13}$$

In a practical implementation of this system, the sequence $f(n)$ would be of finite length and it would often not be necessary to reverse the direction of the input sequence since this does not affect the magnitude of $F[\exp(j\Omega)]$ and $\hat{F}[\exp(j\Omega)]$ and only changes the sign of the phase of $F[\exp(j\Omega)]$.

For $\Omega_a = 0$ and a positive, we note from Fig. 1 that the slope is monotonically decreasing with frequency and consequently, an analysis using the warping given by (10) with $\Omega_a = 0$ will have an analysis bandwidth which increases with frequency. With $\Omega_a \neq 0$, the analysis bandwidth will be minimum around $\Omega = \Omega_a$.

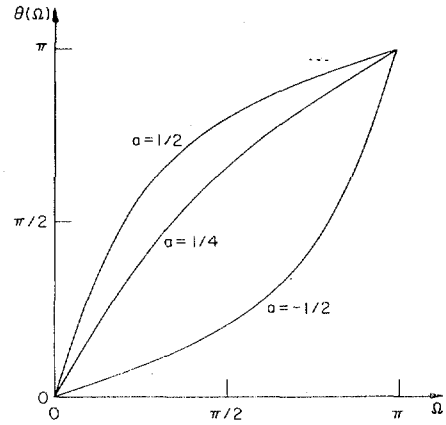

Fig. 1. Frequency transformation of (10) for several values of the parameter a.

To utilize the frequency transformation for vernier analysis we note that with $a > 0$ the curves of Fig. 1 are close to linear in the vicinity of the origin, with slope greater than unity. More generally with the transformation of (10), for $a > 0$, the slope is greater than unity in a frequency range of width $2\cos^{-1}a$ centered at Ω_a. A suitable choice of a and $\hat{B}$, the analysis bandwidth on the $\hat{\Omega}$ axis, allows us to perform a narrow and approximately constant bandwidth analysis around Ω_a at the expense of an increasingly larger bandwidth elsewhere. An example of such an analysis is shown in Fig. 3. In Fig. 3(a) is shown the input sequence consisting of 51.2 ms of speech weighted by a Hanning window. Fig. 3(b) shows the result of applying a 512 point FFT to the sequence in Fig. 3(a). Fig. 3(c) corresponds to applying a 512 point FFT to the sequence obtained by warping the sequence of Fig. 3(a). The parameters used were $a = \frac{1}{2}$ and $\Omega_a = 31\pi/256$. This value of Ω_a corresponds to the location of the arrow in Fig. 3(b). Only a portion of the resulting spectrum is displayed in Fig. 3(c), specifically the portion between the markers in Fig. 3(b). Fig. 3(d) is similar to Figs. 3(b) and 3(c). In Fig. 3(d), a was chosen equal to $\frac{3}{4}$ and the portion of the spectrum of the warped sequence displayed is narrower.

We wish now to compare the analysis as provided by the warping of (10) with constant percentage bandwidth analysis. To present the basis for the comparison procedure it is helpful to refer to Fig. 4, indicating the manner in which a filter with bandwidth $\hat{B}$ is reflected by the curve $\theta(\Omega)$. The bandwidth of the filter applied to the sequence $\hat{f}(n)$ is

$$\hat{B} = \hat{\Omega}_2 - \hat{\Omega}_1 \tag{14}$$

and its center frequency is

$$\hat{\Omega}_c = \tfrac{1}{2}(\hat{\Omega}_2 - \hat{\Omega}_1). \tag{15}$$

The bandwidth and center frequency of the equivalent filter applied to $f(n)$ are

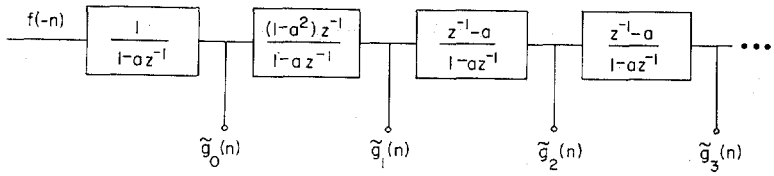

Fig. 2. Cascade chain of networks to implement frequency warping.

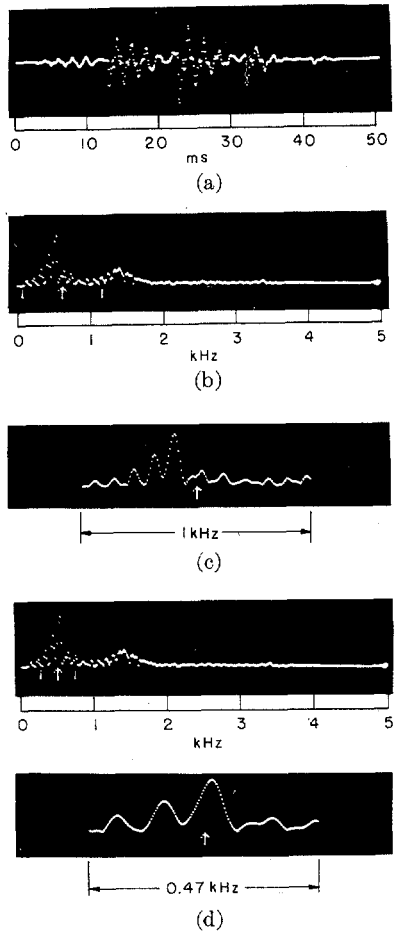

Fig. 3. (a) 51.2 ms of speech weighted by a Hanning window. (b) Spectrum obtained by applying a 512 point FFT to the sequence in (a). (c) Spectrum obtained by applying the FFT to the sequence obtained by warping the sequence in (a) with $a = 1/2$, $\Omega_a = 31\pi/256$. (d) Similar to (b) and (c) but with $a = 3/4$.

$$B = \Omega_2 - \Omega_1 \tag{16}$$

$$\Omega_c = \tfrac{1}{2}(\Omega_2 + \Omega_1). \tag{17}$$

The Q of the effective filters applied to the sequence $f(n)$ is defined as

$$Q = \frac{\Omega_c}{B}. \tag{18}$$

For a constant percentage bandwidth analysis we require that Q be independent of Ω_c and consequently, that B be proportional to Ω_c. That this is in fact so for the logarithmic transformation

$$\hat{\Omega} = a_1 \ln a_2\Omega$$

follows in a straightforward manner.

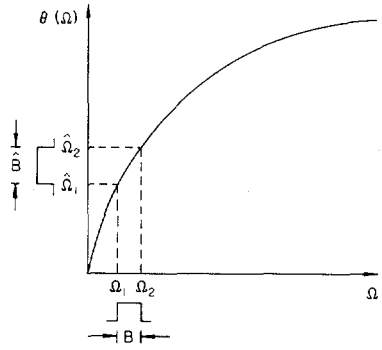

Fig. 4. Transformation of a filter with bandwidth $\hat{B}$ by the warping curve $\theta(\Omega)$.

To evaluate Q for the transformation of (10), we might compute the center frequencies and bandwidths reflected through this frequency transformation. The exact computation of the bandwidths leads to unwieldy expressions and we will instead base the comparison on an approximate analysis. The approximate analysis corresponds to assuming that $\theta(\Omega)$ is linear over an interval with width $\hat{B}$ in $\hat{\Omega}$. With this approximation, $\hat{B}$ and B can be simply related by the slope of $\theta(\Omega)$ at $\Omega = \Omega_c$ and $\hat{\Omega}_c$ and Ω_c are simply related by

$$\hat{\Omega}_c = \theta(\Omega_c). \tag{19}$$

For $a \leq 1/2$, the error is less than 1 percent for $0 \leq \hat{B} \leq 2\pi/32$ and less than 3 percent for $\hat{B} \leq 2\pi/16$. The corresponding maximum errors for $a \leq 15/16$ become, respectively, 3.5 percent and 10 percent.

With the assumption that $\theta(\Omega)$ is linear over the range $\Omega_2 - \Omega_1$ with slope $\theta'(\Omega_c)$, $\hat{B}$ and B are simply related by

$$\hat{B} = B\theta'(\Omega_c). \tag{20}$$

Thus, the Q of the effective filter is

$$Q = \frac{\Omega_c}{B} = \frac{\Omega_c}{\hat{B}}\theta'(\Omega_c). \tag{21}$$

For constant percentage bandwidth, Q is constant, while the Q given in (21) is a function of Ω_c. To compare this with constant Q, we define the error relative to a constant value Q_r as

$$\varepsilon(\Omega_c) = \frac{Q(\Omega_c) - Q_r}{Q_r} \tag{22}$$

where we have denoted the dependence of the error and Q on Ω_c. With the error expressed in this way, Q_r is, of course, arbitrary and the error is therefore dependent on what constant Q value we choose to compare $Q(\Omega_c)$ with. Consequently, it is convenient to display the error in terms of

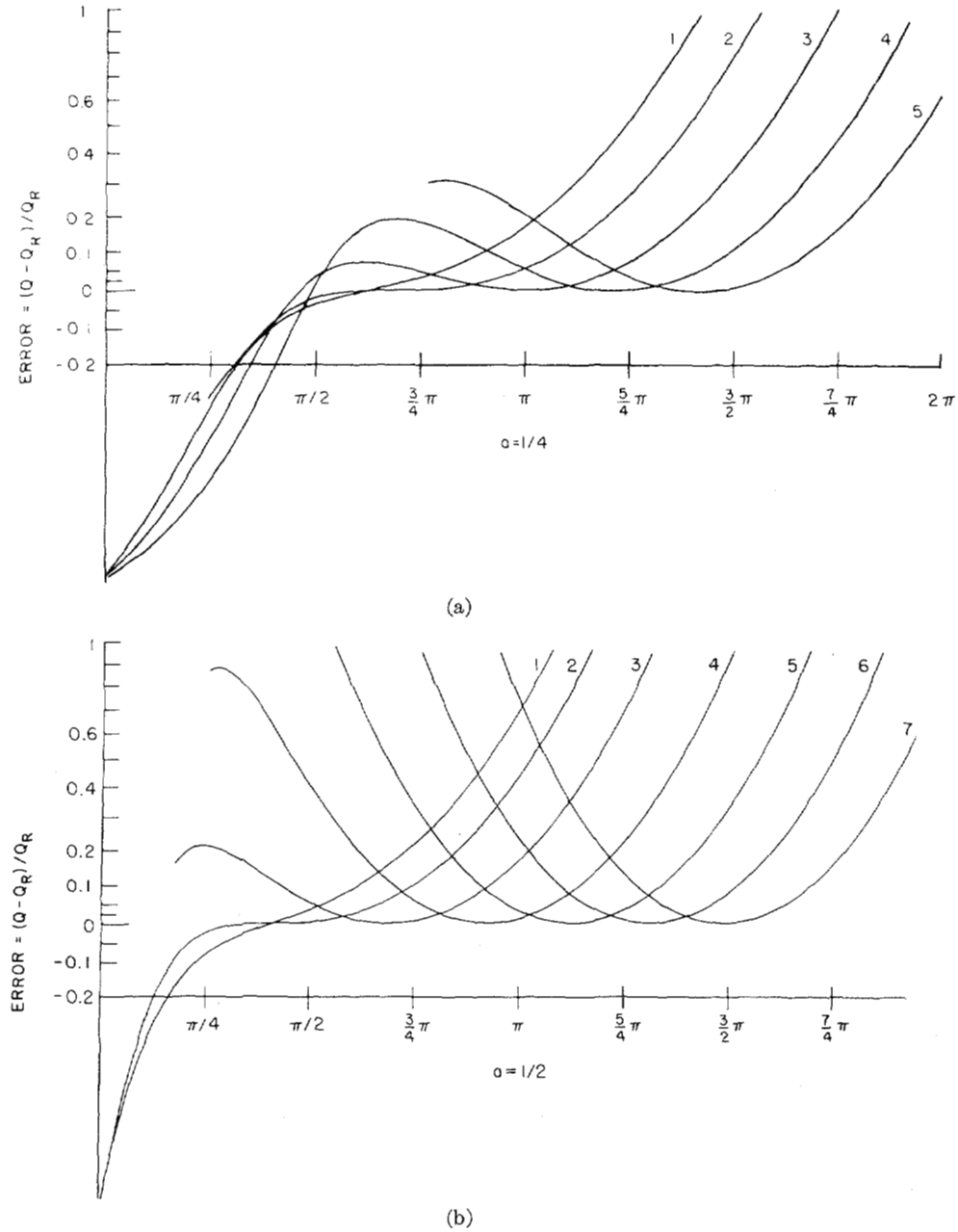

Fig. 5. Error curves for the use of digital frequency warping to approximate constant percentage bandwidth. The parameters for each of the curves are listed in Table I.

$\log [1 + \varepsilon(\Omega_c)]$ since

$$\log[1 + \varepsilon(\Omega_c)] = \log Q(\Omega_c) - \log Q_r. \tag{23}$$

With $\varepsilon(\Omega_c)$ presented in this way, a change in Q_r is reflected by a vertical displacement of the error curve. Since, from (21), $Q(\Omega_c)$ is proportional to $1/\hat{B}$, it is also convenient to consider Q_r to be proportional to $1/\hat{B}$. Thus we express Q_r as $Q_r = C/\hat{B}$.

In Fig. 5, a set of error curves are displayed for different values of a and Ω_a. For each value of a, the different numbered curves presented correspond to a change in Ω_a. It was also convenient for the purpose of displaying these curves, to adjust the vertical position of each curve so that they are tangent to $\varepsilon = 0$. Thus, each curve displayed has associated with it a different value of C.

A table of the values of Ω_a and C for each curve is given in Table I. We note on these curves that for each value of a, those curves which are simple convex curves appear to be quite similar. It has been verified computationally that for values of modulation between those given, linear interpolation provides a close approximation. To discuss how the error curves should be interpreted, let us consider a specific example. Let us assume that we wish to investigate the deviation from constant Q for $a = 1/2$. Referring to the appropriate set of error curves, we note that from curve 3, Fig. 5(b), corresponding to a modulation of zero, it is possible to have a positive error relative to $Q_r = 0.90/\hat{B}$ between 0 and 10 percent in the frequency range $0.42\pi \leq \alpha \leq 0.93\pi$. Alternatively by shifting the same curve downward, we see that it is possible to have an

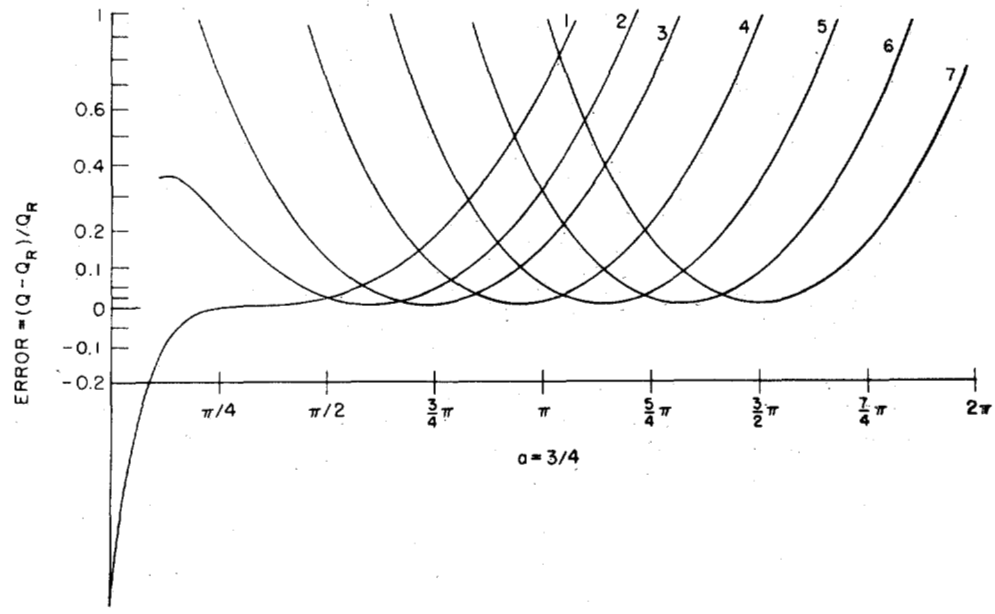

(c)

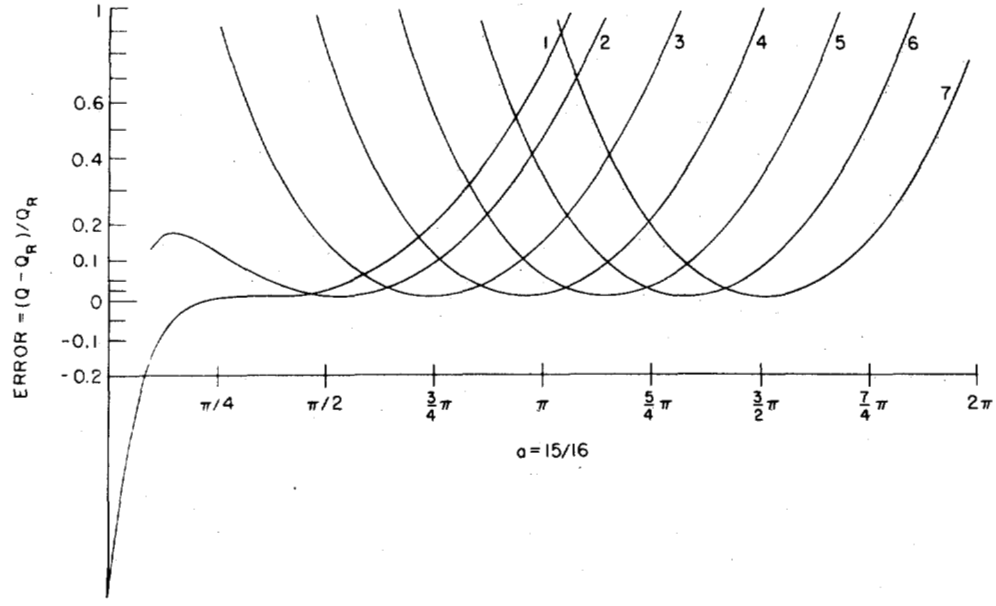

(d)

Fig. 5. (Continued.)

error between ± 10 percent relative to $Q_r = 1/\hat{B}$ in the frequency range $0.26\pi \leq \Omega \leq 1.04\pi$. For $a = 3/4$ with $\Omega_a = 0$, it is possible to have an error between ± 10 percent in the frequency range $0.43\pi \leq \Omega \leq 1.05\ \pi$ with $Q_r = 0.43/\hat{B}$. We note that for Q_r to be same for the two different values of a, $\hat{B}$ can be larger if $a = 1/2$ than if $a = 3/4$. Thus, with $a = 1/2$, a wider bandwidth analysis can be used on the sequence $\hat{f}(n)$.

In a practical setting, we may wish to use the frequency warping to implement an approximation to a constant Q analysis. Given the frequency range to be analyzed and the allowable deviation from constant Q, we can then use the curves of Fig. 5 to choose the parameters a and Ω_a. The design procedure will generally be of a trial and error kind. The choice of Ω_a will generally depend on the range to be analyzed. The parameter a influences that value of Q_r so that as a increases the value of $\hat{B}$ required to approximate a given Q will decrease requiring a finer resolution analysis of $\hat{f}(n)$. At the same time, it is generally possible to extend the frequency range to lower frequencies as a increases.

In the application of the frequency warping technique we have presented, three parameters play a fundamental role: Ω_a, a and $\hat{B}$. While no particular problem is connected with the modulation frequency Ω_a, some comments are in order about a and $\hat{B}$. In the constant Q approximation, values of a close to unity allow us to extend the analysis to low frequencies and small values of $\hat{B}$ are needed to approximate a high Q_r. In the vernier application, we again use large a's and small $\hat{B}$'s. Since a represents the pole location of the digital networks of Fig. 2 and $\hat{B}$ is inversely propor-

TABLE I

	a	Curve No.	Ω_a	C
Fig. 5(a)	1/4	1	0.25	1.4
		2	0.55	1.9
		3	1	2.2
		4	1.5	2.5
		5	2	2.9
Fig. 5(b)	1/2	1	−0.5	0.66
		2	−0.32	0.75
		3	0	0.90
		4	0.5	1.1
		5	1.0	1.2
		6	1.5	1.4
		7	2.0	1.6
Fig. 5(c)	3/4	1	−0.53	0.29
		2	−0.25	0.35
		3	0	0.39
		4	0.5	0.47
		5	1	0.55
		6	1.5	0.63
		7	2	0.70
Fig. 5(d)	15/16	1	−0.57	0.064
		2	−0.4	0.073
		3	0	0.089
		4	0.5	0.11
		5	1	0.12
		6	1.5	0.14
		7	2	0.16

tional to the FFT size, that is to the output length of the warping network, we conclude that in specific applications a very long chain of all-pass networks will be used with the poles close to the unit circle. Consequently, we would expect that with finite register length arithmetic considerations of roundoff noise will play an important role. Thus, the next section is directed toward an analysis of roundoff noise in implementing digital frequency warping.

V. NOISE ANALYSIS OF DIGITAL FREQUENCY WARPING

An implementation of the system of Fig. 2 in terms of multipliers, delays and adders is shown in Fig. 6. Note that, after the first delay, the outputs of this system differ from those of Fig. 2 by a factor of $(1 - a^2)$. Since the system of Fig. 6 implies a simpler hardware structure, it is the system of Fig. 6 that will be analyzed with regard to roundoff noise. The factor $(1 - a^2)$ is easily accounted for in a number of ways such as dividing $\hat{f}(0)$ by $(1 - a^2)$ and applying a scale factor of $(1 - a^2)$ in interpreting the amplitude of the sequence $\hat{f}(n)$.

In analyzing the roundoff noise, we will consider only fixed point arithmetic and assume that rounding is applied after multiplication. The register length will be considered to be b-bits plus sign so that the error due to rounding is between plus and minus $\frac{1}{2} \cdot 2^{-b}$. We will assume that the rounding error can be represented statistically. Thus, white noise generators can be inserted after the multipliers to account for roundoff noise as shown in Fig. 7 [7].

Each of the noise generators $\epsilon_k(n)$ are assumed to be uncorrelated, white, uniformly distributed in amplitude between $\pm\frac{1}{2} \cdot 2^{-b}$ with variance $\sigma_\epsilon^2 = (1/12) \cdot 2^{-b}$. The total noise output at the kth tap is denoted by $\eta_k(n)$.

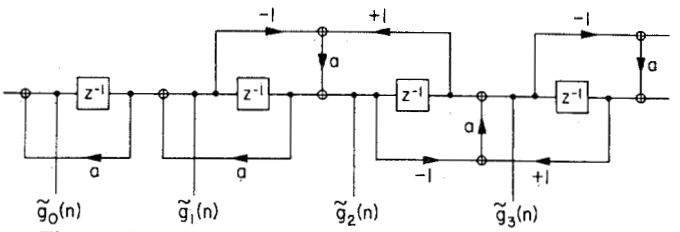

Fig. 6. Block diagram representation of warping network.

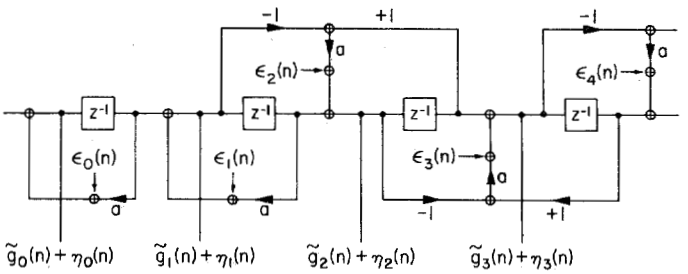

Fig. 7. Network of Fig. 6 with roundoff noise sources inserted.

Let $H_{k,r}(z)$ denote the transfer function from the kth noise source input to the rth output tap where $r \geq k$. Then, since we assume that the $\epsilon_k(n)$ are white and uncorrelated

$$\sigma_\eta^2(r) = \text{var}\,(\eta_r(n)) = \sigma_\epsilon^2 \sum_{k=0}^{r} \frac{1}{2\pi} \int_{-\pi}^{\pi} |H_{k,r}[\exp(j\omega)]|^2 \, d\omega. \quad (24)$$

It can be verified by inspection of Fig. 7 that

$$H_{0,0}(z) = \frac{1}{1 - az^{-1}}$$

$$H_{0,r}(z) = \frac{z^{-1}}{(1 - az^{-1})^2} \left[\frac{z^{-1} - a}{1 - az^{-1}}\right]^{r-1} \qquad r \geq 1$$

$$H_{k,r}(z) = \frac{1}{1 - az^{-1}} \left[\frac{z^{-1} - a}{1 - az^{-1}}\right]^{r-k} \qquad k \geq 1, \qquad r \geq k.$$

Substituting into (24) it then follows that

$$\sigma_\eta^2(0) = \frac{1}{1 - a^2} \sigma_\epsilon^2 \quad (25a)$$

$$\sigma_\eta^2(r) = \left[\frac{a^2(1 + a^2)}{(1 - a^2)^3} + r \frac{1}{1 - a^2}\right] \sigma_\epsilon^2 \qquad r \geq 1. \quad (25b)$$

It is interesting to note that the increase of $\sigma_\eta^2(r)$ with r is relatively mild. If we assume that a is not close to unity then for r large $\sigma_\eta^2(r)$ is approximately proportional to r.

In addition to computing the output noise variance, however, we must consider the effect of limited dynamic range. With limited dynamic range taken into account, we can compute a noise-to-signal ratio at each output node in the network of Fig. 6.

Let us assume that we do not allow the register length to be saturated and that we scale the input to prevent this in the worst case. Applying this constraint, we can compute the variance of the output signal and the noise-to-signal ratio at each stage. Specifically, let $h_{o,k}(n)$ denote

the impulse response of the system from the input to the kth output node and $s_k(n)$ denote the output at the kth node. With input $x(n)$ of finite length N, i.e., $x(n) = 0$ for $n < 0$ and $n \geq N$, it follows that

$$| s_k(n) | \leq \max_{\text{over } n} [x(n)] \sum_{r=0}^{N} | h_{0,k}(r) |.$$

To avoid exceeding the dynamic range, we require that $| s_k(n) | < 1$ for all k, which is guaranteed by scaling the input amplitude so that

$$\max_{\text{over } n} [x(n)] < 1/M$$

where

$$M = \max_{\text{over } k} \sum_{r=0}^{N} | h_{0,k}(r) |.$$

If we assume that the input is white noise uniformly distributed in amplitude between plus and minus $1/M$, then $\sigma_x^2 = 1/(3M^2)$ and the variance of the output signal $s_k(n)$ is

$$\sigma_s^2(0) = \frac{1}{3M^2} \frac{1}{1 - a^2} \tag{26a}$$

$$\sigma_s^2(k) = \frac{1}{3M^2} \frac{a^2(1 + a^2)}{(1 - a^2)^3} \qquad k \geq 1. \tag{26b}$$

Combining (25) and (26), the output noise-to-signal ratio is

$$\frac{\sigma_\eta^2(0)}{\sigma_s^2(0)} = 3M^2\sigma_\epsilon^2$$

$$\frac{\sigma_\eta^2(k)}{\sigma_s^2(k)} = 3M^2\left[1 + k\frac{(1 - a^2)^2}{a^2(1 + a^2)}\right]\sigma_\epsilon^2 \qquad k \geq 1.$$

Thus, the noise-to-signal ratio is a monotonic function of k and consequently, the largest noise-to-signal ratio occurs in the last stage. Then, with $K + 1$ denoting the number of stages in the system, and assuming $K \gg 1$, the noise-to-signal ratio in the last stage can be approximated as

$$\frac{\sigma_\eta^2(K)}{\sigma_s^2(K)} = 3M^2K\frac{(1 - a^2)^2}{a^2(1 + a^2)}\sigma_\epsilon^2. \tag{27}$$

To observe how the noise-to-signal ratio is influenced by the parameters K, a and N, we must consider the influence of these parameters on M. To this end, we consider $S(k)$ defined as

$$S(k) = \sum_{r=0}^{N} | h_{0,k}(r) | \tag{28}$$

so that

$$M = \max_{\text{over } k} [S(k)].$$

Fig. 8 shows a plot of $S(k)$ for several different values of a as a function of N and k. There are a number of trends evident from these plots. First, we note that for a given N and a, $S(k)$ reaches a maximum and then decreases. Furthermore, this maximum reached for k is small compared with N, and the value of k for which $S(k)$ reaches a maximum decreases as a increases. Consequently, it is reason-

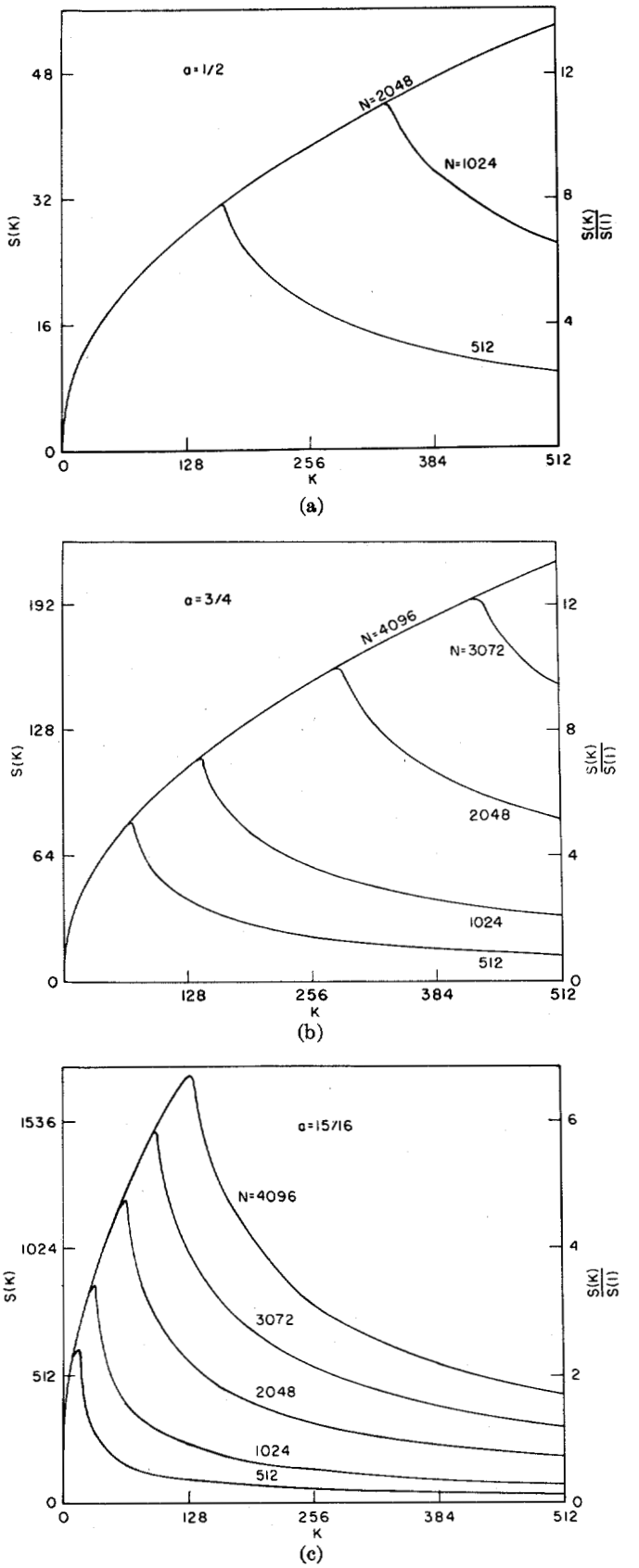

Fig. 8. $S(k)$ for several values of a as a function of N and k. (a) $a = 1/2$. (b) $a = 3/4$. (c) $a = 15/16$.

able to consider M to be independent of K in (27). Thus, from (27), the noise-to-signal ratio does not increase rapidly with K, i.e., it is relatively insensitive to the number of stages.

The above analysis is based on the assumption that at each node the signal value is constrained to be within the limits prescribed by the resister length. A less pessimistic analysis can also be carried out, for which we are willing to permit register saturation to take place a certain percentage of the time. Based on this statistical approach, an approximate analysis can be developed for an input signal which is Gaussian white noise. To develop this analysis let us consider an input signal which is Gaussian white noise with variance σ_f^2. Then the signal at each node is also Gaussian. With $\sigma_s^2(k)$ denoting the variance of the output signal at the kth node, it follows that

$$\sigma_s^2(k) = \sigma_f^2 \frac{1}{2\pi} \int_{-\pi}^{\pi} |H_{0,k}[\exp(j\omega)]|^2 \, d\omega.$$

Thus,

$$\sigma_s^2(0) = \sigma_f^2 \frac{1}{1-a^2}$$

$$\sigma_s^2(k) = \sigma_f^2 \frac{a^2(1+a^2)}{(1-a^2)^3} \qquad k \geq 1.$$

For $a > 1/\sqrt{3}$, $\sigma_s^2(1) > \sigma_s^2(0)$. We note, furthermore, that $\sigma_s^2(k)$ is independent of k for $k > 0$. Thus, let us assume that the maximum output signal variance occurs for $k = 1$. Since we have assumed that the signal is Gaussian, it will exceed the register length a certain percentage of the time and as we scale the input signal the output signal variance is scaled and consequently so is the saturation rate. It is generally convenient to consider this rate to be independent of a in which case we scale σ_f such that $\sigma_s^2(k)$ is constant, i.e., $\sigma_s^2(k) = C$. We would choose the value of C, i.e., of the variance of the Gaussian probability density function, on the basis of the accepted overflow rate, which is represented by the area under the Gaussian curve outside the range $-1 \leq s \leq 1$. With C constant, the maximum output noise-to-signal ratio for $k \geq 1$ is given by

$$\frac{\sigma_\eta^2(k)}{\sigma_s^2(k)} = \frac{1}{C} \sigma_\epsilon^2 \left[\frac{a^2(1+a^2)}{(1-a^2)^3} + k \frac{1}{1-a^2} \right].$$

Thus, the noise-to-signal ratio increases monotonically with k and hence the largest noise-to-signal ratio occurs in the last stage. With $K+1$ stages, and K relatively large, and substituting $\sigma_\epsilon^2 = \frac{1}{12} \cdot 2^{-2b}$, the noise-to-signal ratio in the last stage can be approximated as

$$\frac{\sigma_\eta^2(K)}{\sigma_s^2(K)} = \frac{1}{C} \frac{1}{12} \cdot 2^{-2b} \frac{K}{1-a^2}. \tag{29}$$

If, for example, we consider $a = \frac{3}{4}$ and $K = 2^9$

$$\frac{\sigma_\eta^2}{\sigma_s^2} = \frac{1}{C} \cdot \frac{1}{12} \cdot 2^{-2b} \frac{2^{13}}{7}.$$

In general, we would choose the constant C on the basis of the percentage of the time we are willing to permit the register length to be saturated. For example, let us choose C so that the standard deviation of the output is $\frac{1}{4}$, i.e., $C = 1/16$ and saturation probability is approximately 6×10^{-5}. Then

$$\frac{\sigma_\eta^2}{\sigma_s^2} = \frac{2^{17}}{84} \cdot 2^{-2b};$$

or, in dB,

$$10 \log_{10} \left(\frac{\sigma_\eta^2}{\sigma_s^2} \right) \simeq 31.8 - 6b.$$

Thus, for example with $b = 17$, the noise-to-signal ratio is approximately minus 70 dB. If we choose C instead so that the standard deviation is 1/2, then with $b = 17$, the noise-to-signal ratio is minus 76 dB and the saturation probability is less than 5×10^{-2}.

REFERENCES

[1] J. W. Cooley, P. Lewis, and P. D. Welch, "The fast Fourier transform and its applications," IBM Res. paper, RC-1743, Feb. 9, 1967.

[2] G. C. Carter, C. H. Knapp, and A. H. Nuttall, "Estimation of the magnitude-squared coherence function via overlapped fast Fourier transform processing," *IEEE Trans. Audio Electroacoust.*, vol. AU-21, pp. 337–344, Aug. 1973.

[3] G. Gambardella, "A contribution to the theory of short-time spectral analysis with nonuniform bandwidth filters," *IEEE Trans. Circuit Theory*, vol. CT-18, pp. 455–460, July 1971.

[4] L. R. Rabiner, R. W. Schafer, and C. M. Rader, "The chirp z-transform and its applications," *Bell Syst. Tech. J.*, vol. 48, pp. 1249–1292, May–June 1969.

[5] A. V. Oppenheim, D. H. Johnson, and K. Steiglitz, "Computation of spectra with unequal resolution using the FFT," *Proc. IEEE*, vol. 59, pp. 299–301, Feb. 1971.

[6] A. V. Oppenheim and D. H. Johnson, "Discrete representation of signals," *Proc. IEEE*, vol. 60, pp. 681–691, June 1972.

[7] A. V. Oppenheim and C. J. Weinstein, "Effects of finite register length in digital filtering and the fast Fourier transform," *Proc. IEEE*, vol. 60, pp. 957–976, Aug. 1972.